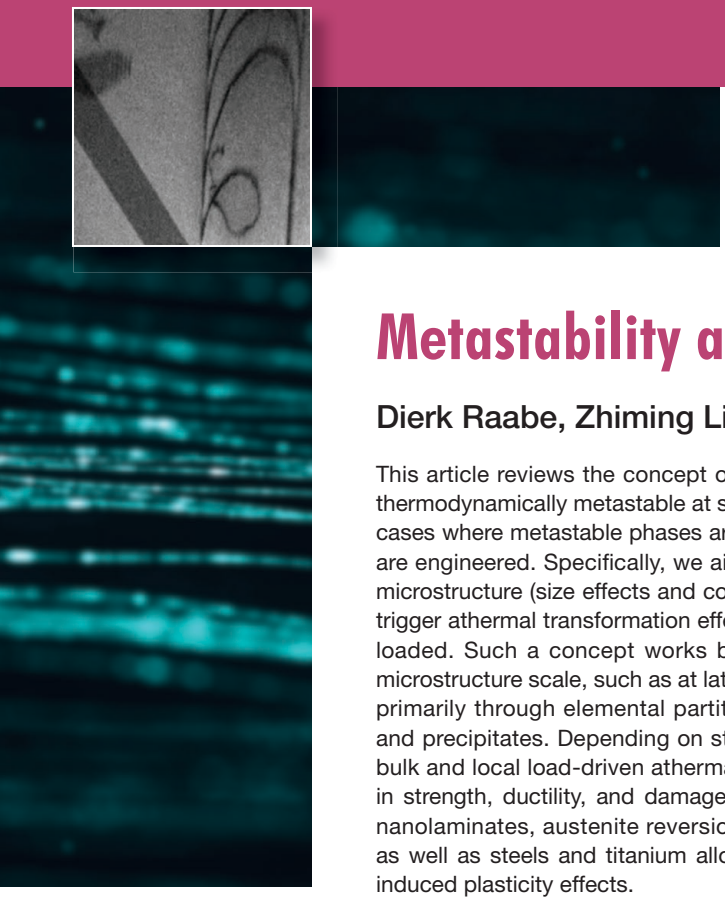


Metastability alloy design

Dierk Raabe, Zhiming Li, and Dirk Ponge

This article reviews the concept of metastability in alloy design. While most materials are thermodynamically metastable at some stage during synthesis and service, we discuss here cases where metastable phases are not coincidentally inherited from processing, but rather are engineered. Specifically, we aim at compositional (partitioning), thermal (kinetics), and microstructure (size effects and confinement) tuning of metastable phases so that they can trigger athermal transformation effects when mechanically, thermally, or electromagnetically loaded. Such a concept works both at the bulk scale and also at a spatially confined microstructure scale, such as at lattice defects. In the latter case, local stability tuning works primarily through elemental partitioning to dislocation cores, stacking faults, interfaces, and precipitates. Depending on stability, spatial confinement, misfit, and dispersion, both bulk and local load-driven athermal transformations can equip alloys with substantial gain in strength, ductility, and damage tolerance. Examples include self-organized metastable nanolaminates, austenite reversion steels, metastable medium- and high-entropy alloys, as well as steels and titanium alloys with martensitic phase transformation and twinning-induced plasticity effects.

Introduction

Most materials are in a thermodynamically metastable state in some stages during synthesis, processing, and service. Microstructure is actually defined as the collective ensemble of all features in a material that are not in thermodynamic equilibrium (i.e., interfaces, dislocations, stacking faults, composition gradients, and dispersed precipitates). These defects, though not in thermodynamic equilibrium, are often retained in materials due to their local mechanical stability and slow relaxation and annihilation kinetics. As these microstructure ingredients endow most materials (e.g., metallic alloys) with their characteristic good load-bearing properties, thermodynamic metastability is a desired material state and the main target behind practically all processing steps that follow primary synthesis. In contrast, alloys in thermodynamic equilibrium are a rare exception with little relevance for applications.

While the arrangement and density of specific defect classes such as dislocations and grain boundaries are frequently addressed topics in microstructure research, less attention has been placed on the role of bulk and local chemical composition and partitioning effects on phase metastability, and its relation to the activation of specific deformation mechanisms. This applies particularly to scenarios where site-specific and self-organized equilibrium segregation to lattice defects changes their local chemical composition, leading to regions of spatially confined metastability. Such a trick, also referred to as segregation engineering,[1–5] can be utilized for enabling activation of athermal transformation effects that are spatially confined only to the metastable defect region. Athermal or diffusionless transformation mechanisms of particular interest in this context include martensitic and twinning-induced plasticity (**Figure 1**). The upper rows in the figure show representative microstructures with the decorating atoms in red. The bottom rows show the local chemical composition. Some of these lattice defect regions become metastable when decorated.

While bulk composition tuning for achieving well-defined phase metastability is a typical design target (e.g., for transformation induced plasticity [TRIP],[6–11] twinning induced plasticity [TWIP],[12–19] duplex,[20] and quench-partitioning steels,[21–24] as well as for some high-entropy alloys[25–47]) it is less commonly used for designing specific chemical decoration states at lattice defects.[1–5,48–50] Spatially confined or compositionally graded metastable states are sometimes accidentally inherited from solidification and processing, but they are usually not engineered.

The aim of the metastability alloy design (MAD) concept lies in the compositional, thermal, and microstructure tuning of metastable phase states for triggering diffusive (e.g., spinodal

Dierk Raabe, Max-Planck-Institut für Eisenforschung, Germany; raabe@mpie.de
Zhiming Li, Department of Microstructure Physics and Alloy Design, Max-Planck-Institut für Eisenforschung, Germany; zhiming.li@mpie.de
Dirk Ponge, Max-Planck-Institut für Eisenforschung, Germany; d.ponge@mpie.de
doi:10.1557/mrs.2019.72

© 2019 Materials Research Society
https://doi.org/10.1557/mrs.2019.72 Published online by Cambridge University Press

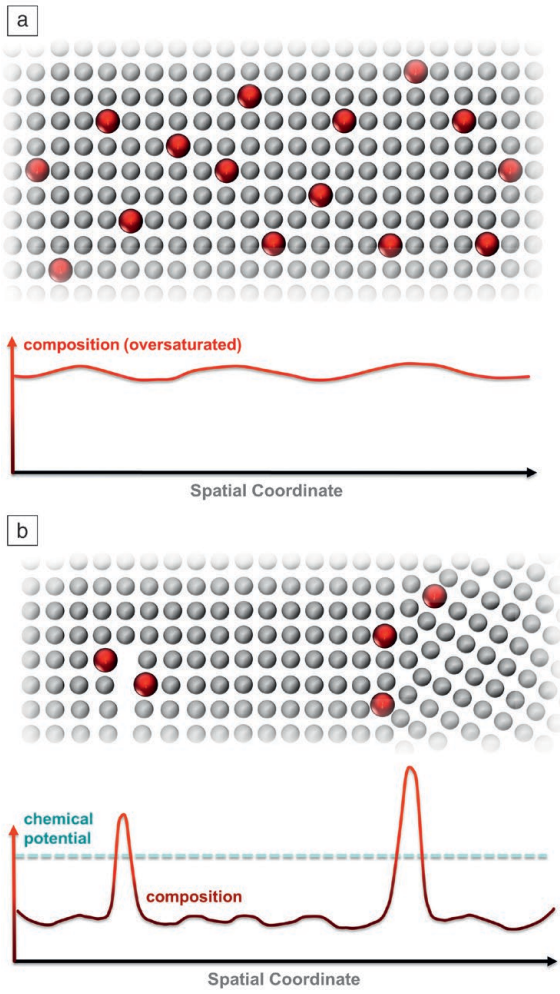


Figure 1. Concept of (a) global (bulk) metastability of an alloy in quenched-in oversaturated state and (b) local metastability, where local chemical segregation to lattice defects can lead to spatially confined stable or metastable states and athermal transformation phenomena when loaded. The latter approach is also referred to as segregation engineering.[1–5] The upper rows show representative microstructures with the decorating atoms in red. The bottom rows show the local chemical composition.

decomposition, discontinuous precipitation, and nucleation) or athermal transformation mechanisms (TRIP and TWIP), particularly when exposed to mechanical, radiation, or thermal loads. Here, we focus particularly on the latter group, namely, athermal transformations in crystalline metastable materials, and show that the effects arising from corresponding composition tuning can reach far beyond the two well-known bulk mechanisms (TRIP and TWIP).

An interesting feature of metastable alloy systems is that the thermodynamic weakness of phases (i.e., their lack of stability) triggers deformation mechanisms, which lead to higher strength and damage tolerance. This is due to the fact that athermal deformation mechanisms are often not commensurate. This means that they require activation of additional deformation mechanisms such as dislocation slip and secondary twinning to accommodate and compensate for local shape and volume mismatch upon deformation. Athermally triggered deformation also introduces a size effect into strain hardening as it occurs in confined regions, entailing high deformation activity, particularly at the interfaces between the host matrix and the transformed volume portion (**Figure 2**). High populations of geometrically necessary dislocations (i.e., dislocation populations accommodating local lattice curvature) are often associated with this confinement.[51] Of particular interest are microstructure design approaches where spatially confined metastability is targeted. In these cases, local stability tuning is achieved through segregation and partitioning to dislocation cores, interfaces, stacking faults, or precipitate phases. When exposed to mechanical stimulus, athermal transformation can be triggered at dimensions as small as a few atomic layers. This gives rise to a double size effect where both the athermally transformed volume and the accommodation plasticity surrounding it are size dependent.

An important feature of (partially) metastable microstructures is that their athermal transformation is activated through deformation. This feature can be utilized to shift the host phase's degree of metastability into a load range where local material weakening sets in. The onset of athermal transformation events then provides additional strain hardening, particularly in those regions and at such load stages where the material is highly deformed and stressed such as shear bands, crack tips, and notches. This strategy provides strain hardening, particularly in weakened microstructure regions where it is most needed. Metastability alloy design can lend a certain self-healing capacity to metallic materials as the associated athermal transformations become active first in locally softened regions that experience high local peaks in deformation and load. Also, they can provide volume mismatch as the volume occupation for the athermally formed new phase is in some cases either larger or smaller than that of the matrix phase, creating local compressive or tensile stress fields. Compressive stresses in particular can assist in closing, blunting, or branching crack tips.[48–50] This applies specifically to alloys that contain interstitial elements that—when frozen-in upon transformation—create tunable volume mismatch between the host and the product phase.

Depending on stability, spatial confinement, misfit, and dispersion, both bulk and local load-driven transformation events can provide substantial gains in strength, ductility, damage tolerance, and functional properties. Examples include self-organized bone-like metastable nanolaminates,[48] nanostructured austenite reversion steels,[49–56] metastable high- and medium-entropy alloys,[25–47] and steels and titanium alloys with nanoscale TRIP and TWIP effects.[57–61]

Effects of bulk metastability on athermal deformation mechanisms

Materials with successfully utilized metastability for microstructure design include alloys undergoing spinodal decomposition, metallic glasses and crystal-glass composites, bulk

https://doi.org/10.1557/mrs.2019.72 Published online by Cambridge University Press

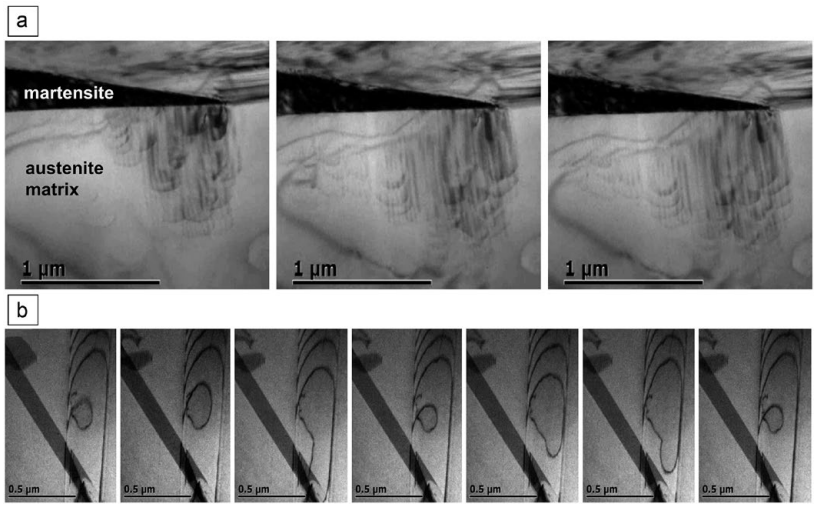


Figure 2. *In situ* transmission electron microscope image sequences revealing the characteristic spatial confinement associated with many athermal deformation effects. (a) TRIP effect where the athermally formed martensite needle (black region) at its tip causes high dislocation multiplication activity in the adjacent metastable austenitic host matrix. The image sequence reveals the increase in dislocation density with increasing local load. (b) Spatially confined dislocation source inside a twin. The image sequence reveals the progress in multiplication of dislocations through a confined source upon *in situ* loading. The results were obtained for a metastable austenitic stainless steel.[8]

TWIP and TRIP steels, shape-memory alloys and TRIP titanium alloys. In TWIP, TRIP, and quench-partitioning steels, face-centered-cubic (fcc) phase stability is typically tuned by adjusting Mn, Ni, C, N, Al, and Si content.[62–68] Interestingly, it was observed that a harmful impurity element such as H can also be used for metastability design—it reduces the stacking-fault energy in Ni and high-entropy alloys, for instance.[69,70]

Depending on the stacking-fault energy, or more generally, on the free energy difference between the matrix phase and the next available (stable or metastable) phase state accessible through athermal transformations, a wide variety of deformation mechanisms triggered under load can be observed. Among these are well-known effects such as formation of hexagonal-close-packed (hcp, ε phase) or body-centered-tetragonal (bct, α′ phase) martensite variants in an fcc host matrix phase or mechanical twin formation. Also included are planar slip-through dislocation core expansions, stacking faults, formation of crystallographic slip bands and their successive dynamic refinement, and partial dislocations, including formation of stair-rod dislocations or the recently observed bidirectional TRIP effect.[71] This mechanism refers to the phenomenon of deformation-driven forward and reverse (bidirectional) martensitic transformation. It occurs when the stacking-fault energy approaches near-zero values and is realized for the fcc-hcp case by the forward and reverse motion of dissociated Shockley partial dislocations. **Figure 3** gives an overview of this rich arsenal of athermal deformation mechanisms occurring in alloys with a metastable fcc matrix structure. The deformation mechanisms are roughly grouped as a function of the free energy difference between the matrix and the next stable or metastable phase. For many fcc alloys (γ), the most frequently occurring adjacent more stable phases are ε (hcp), α (bcc), and α′ (bct) phases. Therefore, in fcc alloys, the reduction in stacking-fault energy can be used as an approximate measure and guideline for designing alloys with desired metastability.

Of particular interest is the situation where the stacking-fault energy of fcc materials approaches near-zero values (e.g., Co close to its allotropic hcp-fcc transformation temperature, and in certain medium- and high-entropy alloys).[71] In this case, the bulk matrix no longer has a preference as to which structure to assume. Local transformation events and microstructure scaling are then dominated by the specific barriers pertaining to the different types of lattice defects that carry the respective transformation mechanism. In these instances, the fcc and hcp phases can coexist and athermally transform into each other upon loading, even in a reversible fashion.[71]

If a bcc/bct phase has a similar free energy, up to three of these phases can simultaneously occur, as has been observed in several stainless duplex steels and TRIP steels where the fcc phase athermally transforms into hcp regions and further into the bcc or bct phase, preferably at the intersection

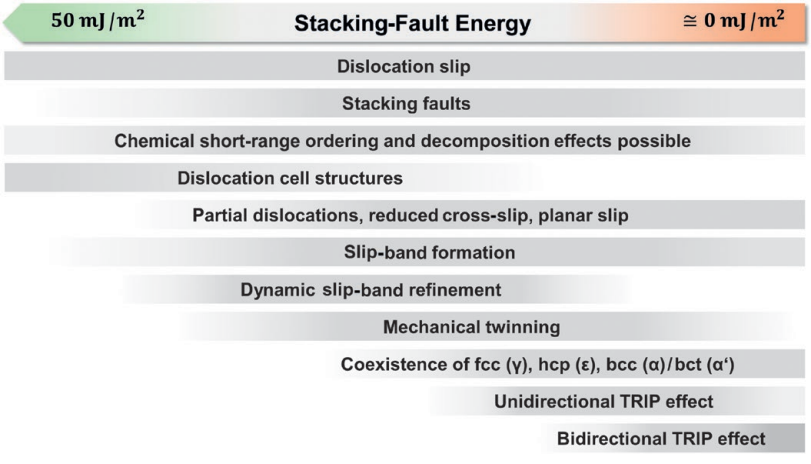


Figure 3. Stacking-fault energy dependence and occurrence of specific deformation effects in metastable alloys with face-centered-cubic (fcc) matrix structure. More intense gray indicates a higher overall contribution to strain and microstructure kinetics. The stacking-fault ranges and associated deformation mechanisms were taken from several works.[6,13–16,19,44,65] Note: hcp, hexagonal close-packed; bcc, body-centered cubic; bct, body-centered tetragonal; TRIP, transformation induced plasticity.

https://doi.org/10.1557/mrs.2019.72 Published online by Cambridge University Press

of two hcp bands.[72–74] In some of these metastable alloys, deformation via athermal transformations leads to complex cascades of metastable transition states. Such effects have some phenomenological similarity with microstructure formation in spinodally decomposing alloys where gradual relaxation from an oversaturated and metastable matrix state can proceed sequentially through multiple transitional phase states.

Bulk metastability alloy design for medium- and high-entropy alloys

Medium- and high-entropy alloys represent a material class particularly well suited for compositional tuning, with the aim to render them thermodynamically metastable. These alloys are amenable to adjusting the stacking-fault energy over a wide range, especially by dropping the entropy maximization rule, thus allowing access to a nearly infinite range of nonequiatomic compositions.[26–46] As previously mentioned, we focus on high-entropy alloy concepts utilizing deformation-stimulated athermal transformations. In this context, several new materials were recently introduced where substantial strain hardening was observed due to athermal transformation of the metastable massive solid-solution matrix phase (**Figure 4**).[25–28,30–33] For example, the phase stability of high- and medium-entropy materials pertaining to the FeCrMnCoNi system, as well as interstitially doped high-entropy alloys,[75] can be well tuned by modifying the ratio among Fe, Mn, Ni, Cr, and Co. Beyond fcc phase-stability trimming, H was also observed to reduce the stacking-fault energy of certain high-entropy alloys with these solid-solution element ratios.[69,70] This effect opens up the opportunity to exploit this otherwise harmful impurity element for metastability tuning of alloys that are exposed to harsh hydrogen-containing environments.

Several studies on these alloy systems revealed that their prevalent deformation mechanisms change when reducing the stacking-fault energy from dislocation shear ($\gtrsim$50 mJ/m^2) toward additional mechanical twinning (20 mJ/m^2 $\leq$ stacking-fault energy $\leq$ 40 mJ/m^2), and further toward dislocation shear plus hcp martensite formation (stacking-fault energy $\leq$ 20 mJ/m^2) (see Figures 3 and 4). Another interesting deformation phenomenon was recently observed when approaching the latter limit of near-zero stacking-fault energy in fcc high-entropy alloys, namely, a bidirectional transformation induced plasticity (B-TRIP) effect. This mechanism describes the joint occurrence of athermal forward transformation from an fcc matrix phase into an hcp nanolaminate structure and the partial dynamic reverse transformation back from hcp to fcc (**Figure 5**).

Similar athermal effects can be achieved in TiZrHf-based medium and high-entropy alloy systems when blending them with bcc stabilizing elements such as Nb, V, Ta, Mo, W, Cr, and Fe, rendering them metastable bcc alloys.[76–78] Athermal transformation sequences in such metastable bcc high- and medium-entropy alloys include formation of bcc twins, athermal bcc-to-hcp phase transformation, hcp twins, and omega phase formation. Chemical ordering and cluster formation may also play a role.[57–61,76–78]

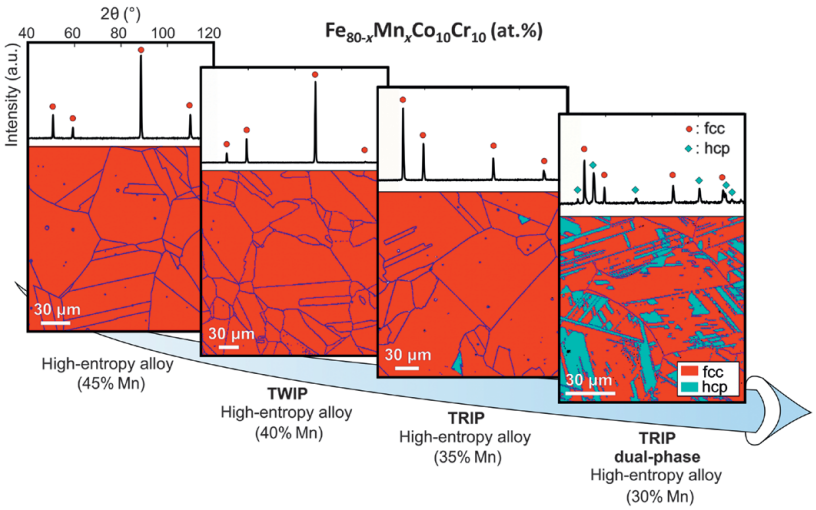


Figure 4. Relaxing the strict configurational entropy maximization rule and favoring instead nonequimolar mixtures opens up an immensely rich composition space for the design of metastable massive solid-solution alloys. This example shows a set of related Fe-Mn-Co-Cr high-entropy alloys with altered Mn/Fe ratio. The compositional adjustment reduces the stacking-fault energy, enabling introduction of several types of phase states and athermal deformation effects.[30] Red color in diffraction patterns (top) and in micrographs (bottom) indicates crystalline regions with face-centered-cubic (fcc) structure and cyan indicates hexagonal-close-packed (hcp) structure. Note: TWIP, twinning induced plasticity; TRIP, transformation induced plasticity.

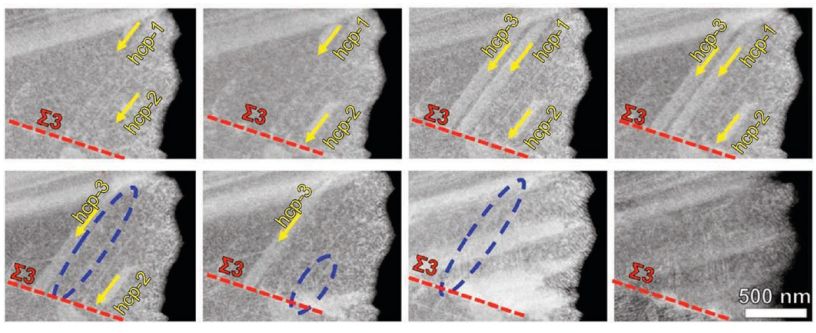


Figure 5. *In situ* low-angle annular dark-field scanning transmission electron microscope observation of a bidirectional transformation induced plasticity effect in a composition-tuned metastable high-entropy alloy. The local strain increases from the top left corner image to the bottom right corner image.[71] Note: hcp, hexagonal close-packed.

https://doi.org/10.1557/mrs.2019.72 Published online by Cambridge University Press

Spatially confined metastability alloy design at decorated lattice defects

Segregation engineering is a concept that renders not the entire host matrix, but only certain regions or phases of an alloy metastable through a corresponding heat treatment and elemental partitioning.[1–5] For some engineering alloys, this approach is well established and has been applied to adjust the stability of adjacent mesoscopic phases such as in quench-partitioning, medium Mn, and duplex stainless steels. In such cases, several size and confinement effects apply. While composition-dependent stacking-fault energy, temperature, and strain rate are the most influential parameters for triggering athermal deformation mechanisms and their activation sequence, specific additional features can be tuned through local chemical partitioning, grain size, texture, and the dislocation substructure. When developing this concept further, it should be emphasized that compositional partitioning generally occurs not only among adjacent mesoscopic phases, but also between the bulk matrix and its lattice defects[48–56] (Figure 1).

Such local chemical decoration effects at lattice imperfections such as dislocations, stacking faults, and grain boundaries can be readily engineered due to the self-organizing nature of the mean-field McLean or Fowler–Guggenheim isotherms.[55] Isotherms are thermodynamic models describing element partitioning between a lattice defect and its adjacent matrix region. The McLean isotherm assumes statistical decoration without any chemical interaction among the segregating atoms. The Fowler–Guggenheim isotherm assumes interaction among the segregating atoms. Typical metallic microstructures represent an array of sinks for trapping solute elements. Each type of lattice defect provides a characteristic density of trapping states and an associated distribution of characteristic trapping energies as shown in Figure 1. When exposed to a heat treatment, the solute elements can redistribute among these multiple traps, which leads to characteristic chemical compositions at the different lattice defects. These individual local decoration states can then lead to individual local metastability states at the defects, capable of producing local phase states that can undergo athermal transformation when exposed to loads.[48–54,79–81]

Compositional adjustment of such local partitioning effects to lattice defects can be readily achieved by adjusting the corresponding heat treatments.[1–3] **Figure 6** shows an example where such local chemical partitioning of Mn to the low-angle lath interfaces of a Fe–Mn-based cubic martensite was

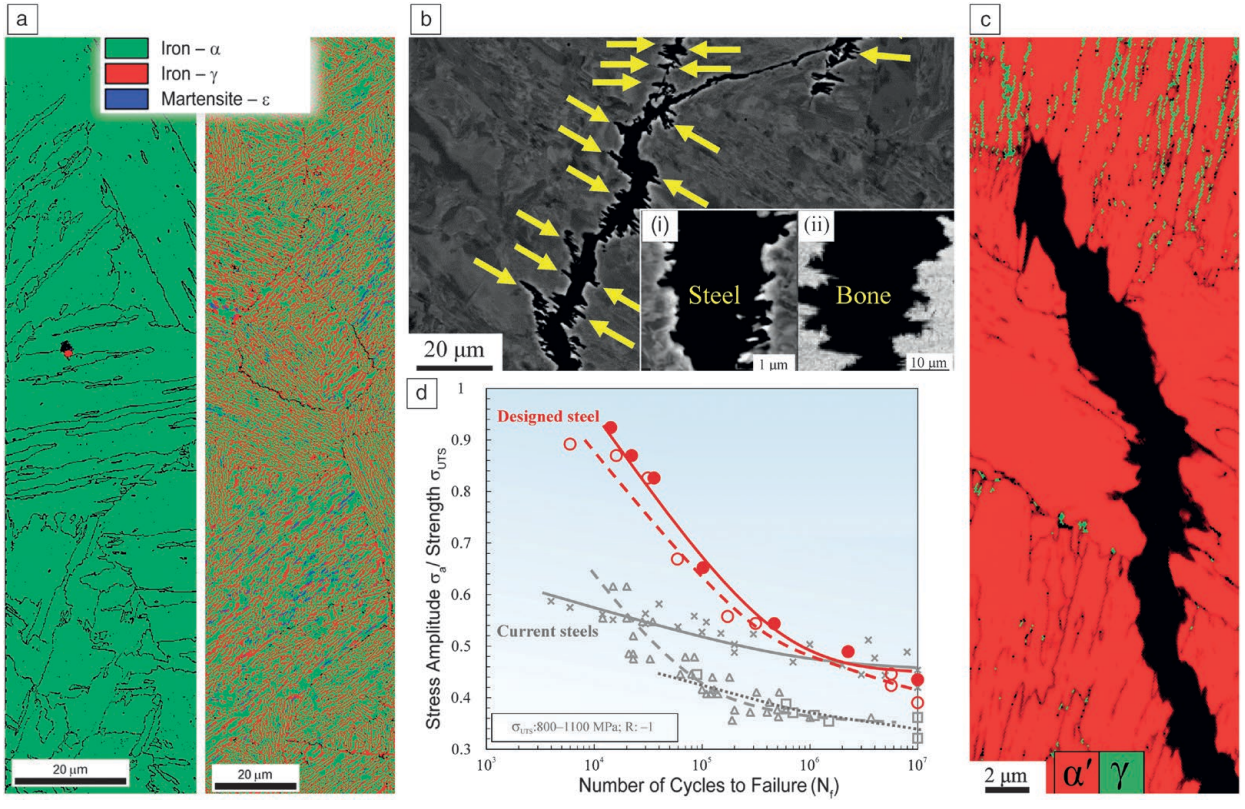


Figure 6. (a) Partitioning of Mn to the low-angle lath interfaces of a Fe-Mn-based cubic martensite was utilized to promote local metastable martensite-to-austenite reversion at these interfaces. (b) Under mechanical fatigue loading, these metastable nanolaminate layers undergo confined transformation from austenite to martensite, (c) triggered by an approaching crack. (b[i]) Zoom-in of the crack in the Fe-Mn-based cubic martensite and (b[ii]) a crack in bone, revealing striking similarity between the two materials. (d) This local athermal transformation lends the material improved resistance to fatigue damage.[48]

https://doi.org/10.1557/mrs.2019.72 Published online by Cambridge University Press

utilized to promote local metastable martensite-to-austenite reversion at these interfaces. These metastable nanolaminate layers undergo spatially confined transformation from austenite back to bcc martensite under mechanical fatigue loading (i.e., triggered by an approaching crack). This confined phase transformation can reduce the crack propagation rate through compressive stresses, crack branching, or blunting, an effect phenomenologically resembling the micromechanics of bone.

Summary and conclusions

Thermodynamic phase metastability can be utilized to make metallic alloys stronger and more ductile, and the types of athermal transformation and accommodation plasticity mechanisms that are responsible were described here. We reviewed two types of approaches. First, we discussed mechanisms and examples of bulk metastability alloy design known from transformation and twinning-induced steels, Ti-alloys, and high-entropy alloys. Next, we showed how spatially confined metastability can be created by heat treatments in which elemental partitioning between the matrix and its lattice defects leads to local metastable phases, a concept also referred to as segregation engineering.

Three trends seem to be particularly promising for further work along these lines. First, bidirectional athermal transformation, occurring when the stacking fault energy approaches near-zero values, leads to an ongoing refinement of the microstructure down to the nanometer regime. This effect leads to a high density of interfaces and stacking faults, hence reducing the mean free dislocation path and thus providing high strength and ductility. A second opportunity in this field lies in the well-targeted segregation at lattice defects, exploiting their usually high density, with the aim to render them metastable and thus amenable for athermal phase transformation when mechanically loaded. A third goal in realizing metastable alloys should be directed at using less expensive alloying elements. Most of the currently developed metastable high- and medium-entropy alloys use expensive alloying elements such as Co and Ni. These could be replaced by much less costly elements, such as Mn, C, or N, which create similar thermodynamic trends.

References

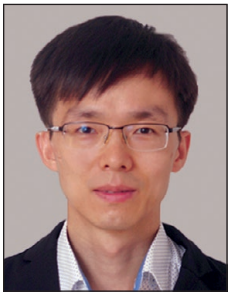
1. D. Raabe, S. Sandlöbes, J. Millán, D. Ponge, H. Assadi, M. Herbig, P.-P. Choi, *Acta Mater.* **61**, 6132 (2013).
2. D. Raabe, M. Herbig, S. Sandlöbes, Y. Li, D. Tytko, M. Kuzmina, P.-P. Choi, *Curr. Opin. Solid State Mater. Sci.* **18**, 253 (2014).
3. M. Kuzmina, D. Ponge, D. Raabe, *Acta Mater.* **86**, 182 (2015).
4. S.K. Makineni, M. Lenz, P. Kontis, Z. Li, A. Kumar, P.J. Felfer, S. Neumeier, M. Herbig, E. Spiecker, D. Raabe, B. Gault, *JOM* **70**, 1736 (2018).
5. Y. Li, D. Raabe, M. Herbig, P.-P. Choi, S. Goto, A. Kostka, H. Yarita, C. Borchers, R. Kirchheim, *Phys. Rev. Lett.* **113**, 106104 (2014).
6. O. Grässel, L. Krüger, G. Frommeyer, L.W. Meyer, *Int. J. Plast.* **16**, 1391 (2000).
7. S. Zaefferer, J. Ohlert, W. Bleck, *Acta Mater.* **52**, 2765 (2004).
8. J. Liu, C. Chen, Q. Feng, X. Fang, H. Wang, F. Liu, J. Lu, D. Raabe, *Mater. Sci. Eng. A* **703**, 236 (2017).
9. D. Raabe, *Acta Mater.* **45**, 1137 (1997).
10. G. Frommeyer, U. Brüx, P. Neumann, *ISIJ Int.* **43**, 438 (2003).
11. J. Han, A.K. da Silva, D. Ponge, D. Raabe, S.-M. Lee, Y.-K. Lee, S.-I. Lee, B. Hwang, *Acta Mater.* **122**, 199 (2017).
12. S. Allain, J.P. Chateau, O. Bouaziz, *Steel Res. Int.* **73**, 299 (2002).
13. O. Bouaziz, S. Allain, C.P. Scott, P. Cugy, D. Barbier, *Curr. Opin. Solid State Mater. Sci.* **15**, 141 (2011).
14. A. Saeed-Akbari, L. Mosecker, A. Schwedt, W. Bleck, *Metall. Mater. Trans. A* **43**, 1688 (2012).
15. I. Gutierrez-Urrutia, D. Raabe, *Acta Mater.* **59**, 6449 (2011).
16. D.R. Steinmetz, T. Japel, B. Wietbrock, P. Eisenlohr, I. Gutierrez-Urrutia, A. Saeed-Akbari, T. Hickel, F. Roters, D. Raabe, *Acta Mater.* **61**, 494 (2013).
17. H. Idrissi, K. Renard, D. Schryvers, P.J. Jacques, *Scr. Mater.* **63**, 961 (2010).
18. I. Gutierrez-Urrutia, S. Zaefferer, D. Raabe, *Mater. Sci. Eng. A* **527**, 3552 (2010).
19. W.S. Choi, S. Sandlöbes, N.V. Malyar, C. Kirchlechner, S. Korte-Kerzel, G. Dehm, B.C. De Cooman, D. Raabe, *Acta Mater.* **132**, 162 (2017).
20. C. Herrera, D. Ponge, D. Raabe, *Acta Mater.* **59**, 4653 (2011).
21. D.V. Edmonds, K. He, F.C. Rizzo, B.C. De Cooman, D.K. Matlock, J.G. Speer, *Mater. Sci. Eng. A* **438**, 25 (2006).
22. J.G. Speer, D.K. Matlock, B.C. De Cooman, J.G. Schroth, *Acta Mater.* **51**, 2611 (2003).
23. Y. Toji, H Matsuda, M. Herbig, P.P. Choi, D. Raabe, *Acta Mater.* **65**, 215 (2014).
24. Y. Toji, G. Miyamoto, D. Raabe, *Acta Mater.* **86**, 137 (2015).
25. Z. Li, C.C. Tasan, K.G. Pradeep, D. Raabe, *Acta Mater.* **131**, 323 (2017).
26. B. Gludovatz, A. Hohenwarter, D. Catoor, E.H. Chang, E.P. George, R.O. Ritchie, *Science* **345**, 1153 (2014).
27. M.J. Yao, K.G. Pradeep, C.C. Tasan, D. Raabe, *Scr. Mater.* **72**, 5 (2014).
28. Y. Deng, C.C. Tasan, K.G. Pradeep, H. Springer, A. Kostka, D. Raabe, *Acta Mater.* **94**, 124 (2015).
29. G. Laplanche, A. Kostka, O. Horst, G. Eggeler, E. George, *Acta Mater.* **118**, 152 (2016).
30. Z.M. Li, K.G. Pradeep, Y. Deng, D. Raabe, C.C. Tasan, *Nature* **534**, 227 (2016).
31. F. He, Z. Wang, Q. Wu, J. Li, J. Wang, C.T. Liu, *Scr. Mater.* **126**, 15 (2017).
32. Z.M. Li, D. Raabe, *JOM* **69**, 2099 (2017).
33. D. Ma, M. Yao, K.G. Pradeep, C.C. Tasan, H. Springer, D. Raabe, *Acta Mater.* **98**, 288 (2015).
34. Y.H. Jo, S. Jung, W.M. Choi, S.S. Sohn, H.S. Kim, B.J. Lee, N.J. Kim, S. Lee, *Nat. Commun.* **8**, 15719 (2017).
35. Z. Wu, H. Bei, G.M. Pharr, E.P. George, *Acta Mater.* **81**, 428 (2014).
36. S. Huang, W. Li, S. Lu, F.Y. Tian, J. Shen, E. Holmström, L. Vitos, *Scr. Mater.* **108**, 44 (2015).
37. S. Huang, H. Huang, W. Li, D. Kim, S. Lu, X. Li, E. Holmström, S.K. Kwon, L. Vitos, *Nat. Commun.* **9**, 2381 (2018).
38. A.J. Zaddach, C. Niu, C.C. Koch, D.L. Irving, *JOM* **65**, 1780 (2013).
39. S.F. Liu, Y.D. Wu, H.T. Wang, J.Y. He, J.B. Liu, C.X. Chen, X.J. Liu, H. Wang, Z.P. Lu, *Intermetallics* **93**, 269 (2017).
40. B. Gludovatz, A. Hohenwarter, K.V.S. Thurston, H.B. Bei, Z.G. Wu, E.P. George, R.O. Ritchie, *Nature Commun.* **7**, 10602 (2016).
41. M.M. Wang, Z.M. Li, D. Raabe, *Acta Mater.* **147**, 236 (2018).
42. C.E. Slone, S. Chakraborty, J. Miao, E.P. George, M.J. Mills, S.R. Niezgoda, *Acta Mater.* **158**, 38 (2018).
43. N.L. Okamoto, S. Fujimoto, Y. Kambara, M. Kawamura, Z.M. Chen, H. Matsunoshita, K. Tanaka, H. Inui, E.P. George, *Sci. Rep.* **6**, 35863 (2016).
44. D. Raabe, C.C. Tasan, H. Springer, M. Bausch, *Steel Res. Int.* **86**, 1127 (2015).
45. L.L. Ma, L. Wang, Z.H. Nie, F.C. Wang, Y.F. Xue, J.L. Zhou, T.Q. Cao, Y.D. Wang, R. Yang, *Acta Mater.* **128**, 12 (2017).
46. Z. Li, F. Körmann, B. Grabowski, J. Neugebauer, D. Raabe, *Acta Mater.* **136**, 262 (2017).
47. J. Moon, Y. Qi, E. Tabachnikova, Y. Estrin, W.M. Choi, S.H. Joo, B.J. Lee, A. Podolskiy, M. Tikhonovsky, H.S. Kim, *Mater. Lett.* **202**, 86 (2017).
48. M. Koyama, Z. Zhang, M. Wang, D. Ponge, D. Raabe, K. Tsuzaki, H. Noguchi, C.C. Tasan, *Science* **355**, 1055 (2017).
49. M. Kuzmina, M. Herbig, D. Ponge, S. Sandlöbes, D. Raabe, *Science* **349**, 1080 (2015).
50. A. Kwiatkowski da Silva, D. Ponge, Z. Peng, G. Inden, Y. Lu, A. Breen, B. Gault, D. Raabe, *Nature Commun.* **9**, 1137 (2018).
51. M. Calcagnotto, D. Ponge, E. Demir, D. Raabe, *Mater. Sci. Eng. A* **527**, 2738 (2010).
52. M.M. Wang, C.C. Tasan, D. Ponge, A. Kostka, D. Raabe, *Acta Mater.* **79**, 268 (2014).
53. M.M. Wang, C.C. Tasan, D. Ponge, A.C. Dippel, D. Raabe, *Acta Mater.* **85**, 216 (2015).
54. M.M. Wang, C.C. Tasan, D. Ponge, A.C. Dippel, D. Raabe, *Acta Mater.* **111**, 262 (2016).
55. R.H. Fowler, E.A. Guggenheim, *Statistical Thermodynamics* (Macmillan, New York, 1939).
56. A. Kwiatkowski da Silva, G. Leyson, M. Kuzmina, D. Ponge, M. Herbig, S. Sandlöbes, B. Gault, J. Neugebauer, D. Raabe, *Acta Mater.* **124**, 305 (2017).
57. J. Zhang, C.C. Tasan, M.J. Lai, A.-C. Dippel, D. Raabe, *Nat. Commun.* **8**, 14210 (2017).
58. M.J. Lai, T. Li, D. Raabe, *Acta Mater.* **151**, 67 (2018).

https://doi.org/10.1557/mrs.2019.72 Published online by Cambridge University Press

59. M.J. Lai, C.C. Tasan, D. Raabe, *Acta Mater.* **111**, 173 (2016).
60. M.J. Lai, C.C. Tasan, J. Zhang, B. Grabowski, L.F. Huang, D. Raabe, *Acta Mater.* **92**, 55 (2015).
61. M.J. Lai, C.C. Tasan, D. Raabe, *Acta Mater.* **100**, 290 (2015).
62. A. Dumay, J.P. Chateau, S. Allain, S. Migot, O. Bouaziz, *Mater. Sci. Eng. A* **483**, 184 (2008).
63. S.T. Pisarik, D.C. Van Aken, *Metall. Mater. Trans. A* **47**, 1009 (2016).
64. M.J. Lai, Y.J. Li, L Lillpopp, D. Ponge, S. Will, D. Raabe, *Acta Mater.* **155**, 222 (2018).
65. D.T. Pierce, J.A. Jimenez, J. Bentley, D. Raabe, C. Oskay, J.E. Wittig, *Acta Mater.* **68**, 238 (2014).
66. H. Springer, D. Raabe, *Acta Mater.* **60**, 4950 (2012).
67. I. Gutierrez-Urrutia, D. Raabe, *Acta Mater.* **60**, 5791 (2012).
68. Z. Li, A. Ludwig, A. Savan, H. Springer, D. Raabe, *J. Mater. Res.* **33**, 3156 (2018).
69. H. Luo, Z. Li, D. Raabe, *Sci. Rep.* **7**, 9892 (2017).
70. H. Luo, W. Lu, X. Fang, D. Ponge, Z. Li, D. Raabe, *Mater. Today* (2018), doi:10.1016/j.mattod.2018.07.015.
71. W.J. Lu, C.H. Liebscher, G. Dehm, D. Raabe, *Adv. Mater.* (2018), doi:10.1002/adma.201804727.
72. S. Mahajan, M.L. Green, D. Brasen, *Metall. Trans. A.* **8**, 283 (1977).
73. J.W. Christian, S. Mahajan, *Prog. Mater. Sci.* **39**, 1 (1995).
74. B. Mahato, S.K. Shee, T. Sahu, S.G. Chowdhury, P. Sahu, D.A. Porter, *Acta Mater.* **86**, 69 (2015).
75. Z. Li, C.C. Tasan, H. Springer, B. Gault, D. Raabe, *Sci. Rep.* **7**, 40704 (2017).
76. O.N. Senkov, J.M. Scott, S.V. Senkova, D.B. Miracle, *J. Alloys Compd.* **509**, 6043 (2011).
77. O.N. Senkov, S.V. Senkova, D.B. Miracle, C. Woodward, *Mater. Sci. Eng. A* **565**, 51 (2013).
78. Z. Lei, X. Liu, Y. Wu, H. Wang, S. Jiang, S. Wang, X. Hui, Y. Wu, B. Gault, P. Kontis, D. Raabe, L. Gu, Q. Zhang, H. Chen, H. Wang, J. Liu, K. An, Q. Zeng, T.G. Nieh, Z. Lu, *Nature* **563**, 546 (2018).
79. H. Springer, M. Belde, D. Raabe, *Mater. Des.* **90**, 1100 (2016).
80. H. Springer, M. Belde, D. Raabe, *Mater. Sci. Eng. A* **582**, 235 (2013).
81. M. Belde, H. Springer, G. Inden, D. Raabe, *Acta Mater.* **86**, 1 (2015). □



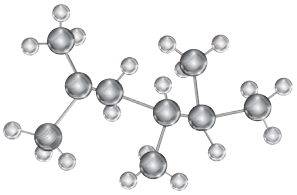
Dierk Raabe is chief executive of the Max-Planck-Institut für Eisenforschung, Germany. He studied music, metallurgy, and metal physics at RWTH Aachen University, Germany. After receiving his Diploma (1990), Doctorate (1992), and Habilitation (1997) degrees in physical metallurgy and metal physics at RWTH Aachen University, he joined Carnegie Mellon University from 1997 to 1999, and joined the Max Planck Society as a director in 1999. His research focuses on the design of metallic alloys, structure–property relations of complex materials, correlative atom probe tomography, and computational materials science. He received the Leibniz-Award, the highest German research award, in 2004 and a European Research Council Advanced Grant in 2012. He is a member of the National Academy Leopoldina and professor at RWTH Aachen and at KU Leuven, Belgium. Raabe can be reached by email at raabe@mpie.de.



Zhiming Li is a project group leader for high-entropy alloys in the Department of Microstructure Physics and Alloy Design at the Max-Planck-Institut für Eisenforschung (MPIE), Germany, and an adjunct professor in the School of Materials Science and Engineering at Central South University, China. He earned his PhD degree in materials science and engineering at Shanghai Jiao Tong University, China, and was a joint doctoral candidate at the University of California, Davis, followed by postdoctoral studies at MPIE. His current research focuses on the development of multicomponent high-entropy alloys, including alloy design, processing, microstructure, and properties. Li can be reached by email at zhiming.li@mpie.de.



Dirk Ponge has been a group leader at the Max-Planck-Institut für Eisenforschung, Germany, since 2001. He studied physical metallurgy and metal physics at RWTH Aachen University, Germany. After completing doctoral (1993) and postdoctoral studies at RWTH Aachen, he became head of the Materials Testing Department and lecturer at the Schweißtechnische Lehr-und Versuchsanstalt Nord, Germany. His research focuses on thermomechanical treatment of steels and compositionally complex alloys, mechanism-based alloy design, and medium-manganese steels. Ponge can be reached by email at d.ponge@mpie.de.



jmr Journal of MATERIALS RESEARCH
2018 PAPER OF THE YEAR
Congratulations!
Huachen Cui, Ryan Hensleigh, Hongshun Chen and Xiaoyu Zheng
Virginia Tech
"Additive Manufacturing and size-dependent mechanical properties of three-dimensional microarchitected, high-temperature ceramic metamaterials"
Published February 14, 2018 - *JMR* Volume 33, Issue 3
This paper will be freely available to the materials community in perpetuity.
mrs.org/jmr

https://doi.org/10.1557/mrs.2019.72 Published online by Cambridge University Press